
Topologically Regularized Multiple Instance Learning to Harness Data Scarcity

Salome Kazemina^{1,2} Carsten Marr^{1†} Bastian Rieck^{1,2†}

Abstract

In biomedical data analysis, Multiple Instance Learning (MIL) models have emerged as a powerful tool to classify patients’ microscopy samples. However, the data-intensive requirement of these models poses a significant challenge in scenarios with scarce data availability, e.g., in rare diseases. We introduce a topological regularization term to MIL to mitigate this challenge. It provides a shape-preserving inductive bias that compels the encoder to maintain the essential geometrical-topological structure of input bags during projection into latent space. This enhances the performance and generalization of the MIL classifier regardless of the aggregation function, particularly for scarce training data. The effectiveness of our method is confirmed through experiments across a range of datasets, showing an average enhancement of 2.8% for MIL benchmarks, 15.3% for synthetic MIL datasets, and 5.5% for real-world biomedical datasets over the current state-of-the-art.

1. Introduction

Multiple Instance Learning (MIL) is a variant of weakly-supervised learning that operates without annotations for individual data samples. In MIL, each *bag*, i.e., a group of instances, is assigned a *single* label (Lu et al., 2020). A bag is labeled positive if it contains at least one positive instance and negative otherwise. MIL-based deep classifiers require substantial training data for optimal performance, primarily due to the complexities inherent to backpropagation and the challenge of addressing diversities within bags: The loss signal must effectively navigate through the aggregation function that ensures precise training of the model to

^{*}Equal supervision ¹Institute of AI for Health, Helmholtz Zentrum München, German Research Center for Environmental Health, Neuherberg, Germany ²TUM School of Computation, Information and Technology, Technical University of Munich, Munich, German. Correspondence to: Bastian Rieck <bastian.rieck@helmholtz-munich.de>, Carsten Marr <carsten.marr@helmholtz-munich.de>.

represent each instance.

MIL classifiers are widely used for biomedical applications like pathology and hematology disease classification (Chen et al., 2022; Hehr et al., 2023; Kazemina et al., 2022; Li et al., 2021; Sadafi et al., 2020; Shao et al., 2021; Wagner et al., 2023; Zhang et al., 2022). Here, representing individual instances properly is pivotal in interpreting the model’s reliability, especially in clinical decision-making contexts. Unfortunately, data scarcity is a common problem in biomedical scenarios, particularly when dealing with rare diseases like rare anemias. In such cases, the need for MIL-based training approaches that operate in the scarce-data regime is paramount.

Improving MIL under data scarcity necessitates leveraging additional structure from data via inductive biases (Goyal & Bengio, 2022). Being able to capture fundamental organizational principles of data at multiple scales, topological algorithms* recently arose as a source of such inductive biases, permitting the integration into deep learning models (Hensel et al., 2021). The primary appeal of such algorithms lies in their robustness to noise and perturbations, resulting in *stable multi-scale representations*. When a pronounced geometrical-topological signal is present in the data, these algorithms improve interpretability, generalizability, and predictive performance (Horn et al., 2022; Waibel et al., 2022), even in the presence of *singular structures*, which preclude the use of standard techniques (von Rohrscheidt & Rieck, 2023).

We introduce *Topologically-Regularized Multiple Instance Learning (TR-MIL)*, a data-centered solution to address the challenges of training MIL with scarce training data. By leveraging multi-scale shape descriptors on the level of MIL bags, we develop a novel regularization scheme that ensures the preservation of crucial geometrical-topological information in the latent space of our model (see Figure 1 for a schematic overview). Our regularization method improves generalization performance, exhibiting higher accuracy and robustness, as well as improved adaptability to data-scarcity. The **main contributions** of our work are:

- We introduce TR-MIL, the first method to improve

*Despite their name, these algorithms also capture geometrical aspects of data, but we will refrain from writing *geometrical-topological algorithms* for brevity.

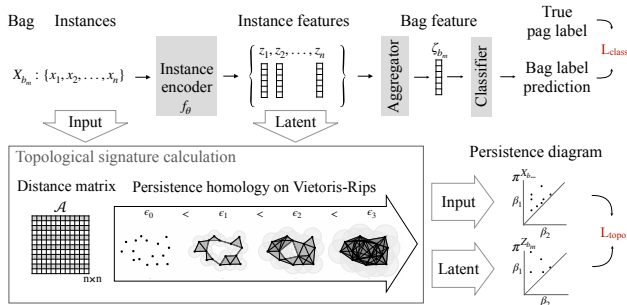


Figure 1: Topologically Regularized Multiple Instance Learning (TR-MIL): We calculate the distance matrix of input instances x_i inside each bag X_{b_m} . Subsequently, we apply persistent homology based on the Vietoris-Rips complex, by treating each bag of n instances as a point cloud. We employ the same process for the latent feature vectors of each bag. Generating shape descriptors (*persistence diagrams*) for both the latent space and the image space representations of the bag, we calculate a topological regularization loss (L_{topo}) and combine it with the standard MIL loss (L_{class}).

generalizability of MIL trained with scarce data.

- We demonstrate that maintaining the topological bias inherent in a bag’s data distribution enhances the performance of MIL classifiers trained with variant amounts of data.
- TR-MIL adapts to any MIL model aggregation strategy.
- TR-MIL outperforms state-of-the-art on MIL benchmarks.
- TR-MIL outperforms the state-of-the-art on rare anemia classification.

2. Background

MIL Architectures. MIL architectures typically comprise three key components: an instance encoder, an aggregation function, and a classifier head (Figure 1). Given a collection of bags b_1, \dots, b_M , each bag contains a set of instances, represented as $X_{b_m} := \{x_1, \dots, x_n\}$ with n denoting the number of instances in the bag. An instance encoder f_θ with parameters θ transfers instance data into a latent space, yielding feature vectors $z_i := f_\theta(x_i)$. The aggregation function then creates a global representation of a bag z_{b_m} from these embedded instances. Finally, this bag representation is passed through a classifier head, which predicts the overall label of the bag.

Geometry & Topology. Our work is based on recent advances in topological machine learning (Hensel et al., 2021), a nascent field that aims to leverage geometry and topology from data to elicit improved representations. We employ *persistent homology*, a technique for calculating multi-scale geometrical-topological information from data (Edelsbrun-

ner & Harer, 2009). Persistent homology considers data to be a point cloud (Figure 1, using a metric (e.g., Euclidean distance) to assess its multi-scale shape information. This includes topological information like connected components, cycles, and higher-dimensional voids in addition to geometrical information like curvature or convexity (Bubenik et al., 2020; Turkes et al., 2022). Such information is collected in a set of *persistence diagrams*, i.e., multi-scale topological descriptors. These descriptors are calculated by approximating the data in terms of a simplicial complex, i.e., a generalized graph, typically based on distance functions like the Euclidean distance. Recent work proved that persistent homology can be integrated with deep learning models, leading to a new class of hybrid models that are capable of capturing topological aspects of data. Such models have shown exceptional performance as regularization terms in different applications (Chen et al., 2019; Vandaele et al., 2022; Waibel et al., 2022).

3. Related Work

MIL aggregation functions can take simple forms, such as max or average pooling, or more complex forms, like attention-based pooling, as commonly used in various MIL models in the literature (Ilse et al., 2018; Kazeminiya et al., 2022; Li et al., 2021; Shao et al., 2021; Zhang et al., 2022; Zhao et al., 2023). Simple aggregation functions are computationally efficient and easy to implement but may overlook instance-level information, whereas complex forms offer a more detailed understanding of relevant instances at the cost of increased computational complexity. Attention-based pooling amplifies the learning signal for important instances, ensuring improved classification performance, even when only a subset of positive instances is distinguished. However, in scenarios where instance-level performance is crucial, the attention-based pooling approach may lack the necessary reliability, as it does not uniformly enhance expression across all instances. To overcome this limitation, Du et al. (2023) recently introduced a regressor-guided aggregator that removes learnable attention parameters and rectifies the inference process, thereby enhancing the direct passage of the learning signal through the encoder. Although this state-of-the-art approach significantly refines instance-level representation and enhances overall MIL performance, it still faces challenges when dealing with scarcity of training data. In such scenarios, the regressor-guided aggregator may struggle to accurately capture and represent the nuanced variations within the data, leading to potential limitations in model generalization and reliability. This is particularly evident in settings where the data lacks diversity or sufficient examples of certain classes, making it difficult for the model to learn and generalize effectively. To address these limitations, we introduce topological regularization, establishing a more robust and rational inductive bias that enhances the

model’s overall performance and generalization.

4. Methods

Our approach treats each bag as a point cloud in a high-dimensional space whose geometrical-topological features should be adequately captured by the model. Each instance influences the bag’s ‘shape,’ with positive instances notably altering its shape in comparison to the distribution of negative samples. We thus need a descriptor that captures the characteristics of a point cloud, while remaining stable to perturbations and invariant under transformations like translations and rotations that are irrelevant for determining the overall shape. Persistent homology provides such a suitable descriptor; Sheehy (2014) demonstrates that critical topological-geometrical features captured by persistent homology are approximately even under projections or embeddings of the data, making it highly robust. The calculation of persistent homology only requires a choice of distance metric. While our framework remains agnostic to the specific choice of distance metric, we opted to use the per-pixel Euclidean distance here since it is straightforward to calculate. This enables us to transform the point cloud of a bag X_{b_m} into a distance matrix $A^{X_{b_m}}$ (see Figure 1). Next, we use the distance matrix A representing the bag’s point cloud and calculate its Vietoris-Rips complex, $\text{VR}(A, \epsilon)$, where points are connected if they lie within a distance ϵ of each other, i.e.,

$$\text{VR}(A, \epsilon) = \{\sigma \subseteq A \mid \forall a_i, a_j \in \sigma, d(a_i, a_j) \leq \epsilon\}. \quad (1)$$

Here, $d(a_i, a_j)$ denotes the distance between points a_i and a_j in A . The topology of VR changes as we vary ϵ . Formally, this leads to a filtration of simplicial complexes $\{\text{VR}(A, \epsilon_0), \text{VR}(A, \epsilon_1), \dots, \text{VR}(A, \epsilon_m)\}$, with an ordered sequence of distance thresholds $0 = \epsilon_0 < \epsilon_1 < \dots < \epsilon_m$ (Figure 1). Persistent homology tracks the ‘birth’ and ‘death’ of topological features across this sequence, represented in a persistence diagram by points (β_1, β_2) , where $\beta_1 = \epsilon_i$ and $\beta_2 = \epsilon_j$. This diagram constitutes a summary of the shape of each bag, measured by multi-scale topological features like connected components (0D), loops (1D), and voids (2D) (Figure 1) and yields a set of d -dimensional persistence diagrams, described in the form of *persistence pairings* $\pi^{X_{b_m}}$ of points in the input space, representing the bag’s topological signature. While our method generalizes to features of arbitrary dimensions, we focus on connected components for computational considerations.

Our objective is to inject this signature as an inductive bias into the model to enhance its robustness and predictive performance. Thus, we capture the distance matrix $A^{Z_{b_m}}$ and signature of the bag’s point cloud in the latent space $\pi^{Z_{b_m}}$ and define a loss term to penalize the encoder f_θ for any inconsistency in preserving the bag’s signature during projection from input to latent space. To this end, we utilize

the topological regularization loss proposed by Moor et al. (2020), which addresses the challenge of backpropagating through topological descriptors. This approach retains topological features in the input space as prominent features in the latent representation by defining a loss $L_{X_{b_m} \rightarrow Z_{b_m}}$. To enhance stability in the model’s outcomes, it simultaneously penalizes topological features within the latent space that lack corresponding importance in the input domain by $L_{Z_{b_m} \rightarrow X_{b_m}}$. The final topological regularization loss is defined as

$$L_{\text{topo}} := L_{X_{b_m} \rightarrow Z_{b_m}} + L_{Z_{b_m} \rightarrow X_{b_m}}, \quad (2)$$

where

$$L_{X_{b_m} \rightarrow Z_{b_m}} := \frac{1}{2} \|A^{X_{b_m}} [\pi^{X_{b_m}}] - A^{Z_{b_m}} [\pi^{X_{b_m}}]\|^2, \quad (3)$$

and

$$L_{Z_{b_m} \rightarrow X_{b_m}} := \frac{1}{2} \|A^{Z_{b_m}} [\pi^{Z_{b_m}}] - A^{X_{b_m}} [\pi^{Z_{b_m}}]\|^2, \quad (4)$$

with $\pi^{X_{b_m}}$ and $\pi^{Z_{b_m}}$ denoting the persistence pairing of topological features in the input space and the latent space, respectively.

Our framework is flexible to integrate any aggregation function for representing the whole bag ζ_{b_M} . With this, the classifier head, incorporating a linear regressor and softmax functions, assigns the bag’s label based on its refined representation. Similar to standard MIL models, we train the MIL classification head using cross-entropy loss, computed based on the divergence between the predicted label of the bag and its corresponding ground truth label, thereby guiding the model towards accurate bag-level predictions. Our formulation also gives rise to a variant of a multi-classifier head approach like the auxiliary loss that Sadafi et al. (2020) proposed. The final loss of topologically-regularized MIL (TR-MIL) framework L_{total} is the weighted sum of the MIL classification loss L_{class} and topological regularization term L_{topo} :

$$L_{\text{total}} = L_{\text{class}} + \lambda L_{\text{topo}}, \quad (5)$$

where λ is a hyperparameter to adjust the influence of the topological regularization loss (Appendix A.1) presents more details of MIL architecture examples.

Complexity and Parameters. The computational complexity involved in calculating certain topological features aligns more closely with the rate of the inverse Ackermann function (Cormen et al., 2022), which increases significantly slower compared to the rate of increasing n . Therefore, the computational complexity of the topological signature calculation of a bag containing n instances is dominated by the calculation of pairwise distances, i.e., $\mathcal{O}(n^2)$, considering that we only capture 0-dimensional topological features. The topological signature calculation does not introduce any additional learnable parameters, thereby keeping the model’s parameter size unchanged. It merely introduces

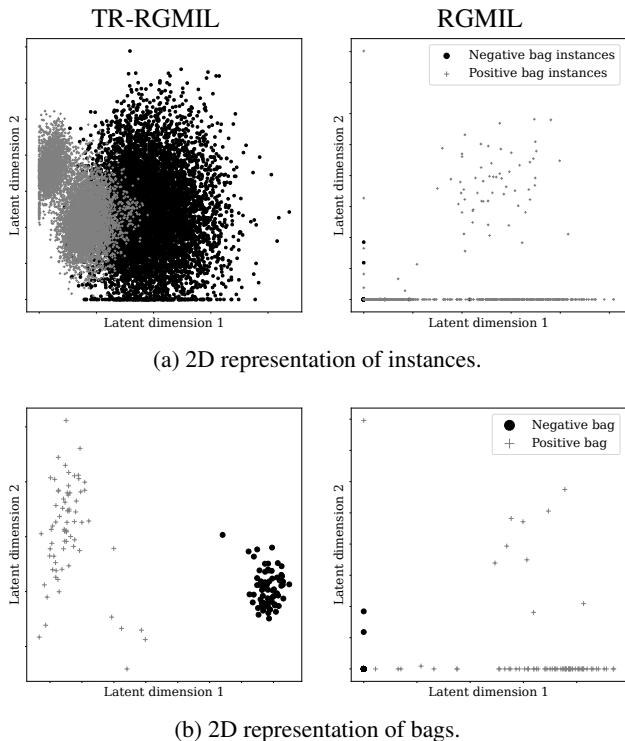


Figure 2: TR-RGMIL preserves the topology of toy instances sampled from a hypersphere when projecting them to the 2D latent (a). It leads to a more distinguished latent representation of bags (b) and 30% higher classification accuracy compared to RGMIL.

one topological regularization loss and one hyperparameter, denoted as λ .

Limitations. The primary limitation of our approach is that the calculation of topological features does *not* exhibit favorable scaling parameters in case higher-order topological features are required. While our implementation supports topological features of arbitrary dimension, their calculation scales progressively worse; connected components, i.e., 0-dimensional features, can still be efficiently calculated (see previous paragraph), but higher-order features may prove limiting. We plan on investigating mitigation strategies in future work, using, e.g., approximate filtrations (Sheehy, 2013) or distributed computations (Wagner et al., 2021).

Toy dataset. As an illustrative example, we consider a toy dataset, where negative instances are sampled from a 100-dimensional random space and positive instances are sampled from the surface of a 100-dimensional sphere as a known geometrical object. To satisfy the positive bag definition of MIL, the sphere overlaps with the space of random negative instances. We consider a simple 2-layer en-

coder projecting instances from the 100-dimensional space to a visualizable 2-dimensional representation (see Table 3). We apply our framework utilizing regressor-guided aggregation (Du et al., 2023) to the dataset. We chose this aggregation function due to its demonstrated superiority in instance-level performance. Figure 2 illustrates the resulting instance and bag representations, contrasting the scenarios with and without topological regularization. TR-RGMIL preserves the topology of positive instances, resembling a circle, as the expected 2D projection of a hypersphere. As a result, the aggregated bag’s latent is more distinct, leading to a higher classification accuracy (RGMIL and TR-RGMIL yield 0.55 ± 0.05 and 0.8 ± 0.22 accuracy, respectively, averaged in 5 runs).

5. Experiments

We evaluate TR-MIL on different datasets: MIL benchmarks, synthetic MIL datasets, and a real-world biomedical dataset for anemia classification.

5.1. MIL Benchmarks

We evaluate TR-MIL on five classic MIL benchmark datasets. These include three image-based datasets (FOX, TIGER, and ELEPHANT), each comprising 200 bags, introduced by Dietterich et al. (1997). For these datasets, instead of actual images, we only have extracted features from tiled image patches (instances) representing parts of an image. Additionally, we employ MUSK1 and MUSK2 datasets, introduced by Andrews et al. (2002), which contain data on 92 and 102 molecules, respectively. In these datasets, each molecule is represented by a bag of instances, with each instance corresponding to a different molecular conformation. The number of instances per bag ranges from as few as 1 to as many as 1044, providing a comprehensive assessment of our model’s adaptability and robustness across different scales of data representation.

We utilized an identical encoder architecture to clarify and ensure an equitable comparison with the existing state-of-the-art MIL method (RGMIL). This architecture includes 2 linear layers with a ReLU activation, projecting input features into a 512-dimensional space for both layers. The primary modification in our setup is integrating a topological signature calculator into the input and instance encoder.

The original RGMIL model used 231 features for FOX, TIGER, and ELEPHANT datasets and 167 features for MUSK1 and MUSK2 datasets, including a last feature representing the repeated label of the bag for each instance. However, in our re-implementation, we followed the standard benchmark settings of 230 and 166 features for the respective datasets to align with previous works and provide a comprehensive comparison (see Table 4). We run both the

Table 1: Topological regularization improves the classification performance of RGMIL (SOTA) on MIL benchmarks. Among previous methods, we specifically reimplemented RGMIL for our analysis. Other results (gray) are collected from papers proposed by Ilse et al. (2018) (APMIL and GAPMIL), Yan et al. (2018) (DPMIL), Li et al. (2021) (DSMIL), Huang et al. (2022) (BDRMIL), and Du et al. (2023) (RGMIL).

| Method | MUSK1 | MUSK2 | FOX | TIGER | ELEPHANT |
|-----------------|--------------------|--------------------|--------------------|--------------------|--------------------|
| APMIL (2018) | 0.892±0.040 | 0.858±0.048 | 0.615±0.043 | 0.839±0.022 | 0.868±0.022 |
| GAPMIL (2018) | 0.900±0.050 | 0.863±0.042 | 0.603±0.029 | 0.845±0.018 | 0.857±0.027 |
| DPMIL (2018) | 0.907±0.036 | 0.926±0.043 | 0.655±0.052 | 0.897±0.028 | 0.894±0.030 |
| DSMIL (2021) | 0.932±0.023 | 0.930±0.020 | 0.729±0.018 | 0.869±0.008 | 0.925±0.007 |
| BDRMIL (2022) | 0.926±0.079 | 0.905±0.092 | 0.629±0.110 | 0.869±0.066 | 0.908±0.054 |
| RGMIL (2023) | 0.940±0.070 | 0.920±0.106 | 0.714±0.107 | 0.842±0.088 | 0.915±0.042 |
| TR-RGMIL (ours) | 0.946±0.078 | 0.970±0.042 | 0.747±0.054 | 0.961±0.040 | 0.941±0.054 |

RGMIL and TR-RGMIL models 5 times, applying 10-fold cross-validation and reporting the average optimal performance of the model during the training. When using this instance feature vector, we observed a decline in RGMIL’s performance, with TR-RGMIL still outperforming all other methods in all five standard MIL benchmarks (Table 1).

Our experiments reveal that the RGMIL model is prone to overfitting if no topological regularization is being used. This phenomenon is characterized by the MIL classifier exhibiting its best performance during the initial epochs of training. Topological regularization effectively mitigates this overfitting issue (Figure 7).

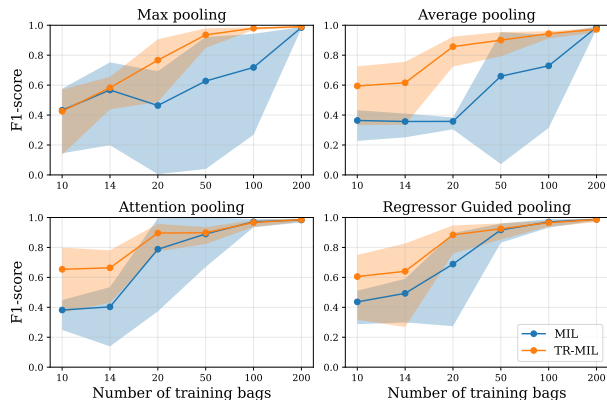
5.2. Synthetic Datasets

For evaluating the robustness of TR-MIL framework across varied MIL problem definitions, including instance image complexity, number of training bags, and bag sizes, we draw on the methods outlined by Ilse et al. (2018). To consider the inherent complexity of instance images, we create two synthetic datasets: the first comprising MNIST images as instances (MIL-MNIST), and the second bags of Fashion-MNIST images (Xiao et al., 2017) as instances (MIL-FashionMNIST), providing a more challenging scenario with complex visual data. In MIL-MNIST, the digit “9” is considered a positive instance, while all other digits are considered negative instances. In MIL-FashionMNIST, the label “Dress” is considered a positive instance, while other labels showcase negative instances. We construct distinct training datasets containing a total number of 10, 14, 20, 50, 100, and 200 bags to evaluate the influence of the quantity of training data. Additionally, we explore different amounts of instances per bag, sampling them from Gaussian distributions with mean and standard deviations defined as (10, 2), (50, 10), and (100, 20), respectively. Positive bags are defined as those containing at least one positive instance,

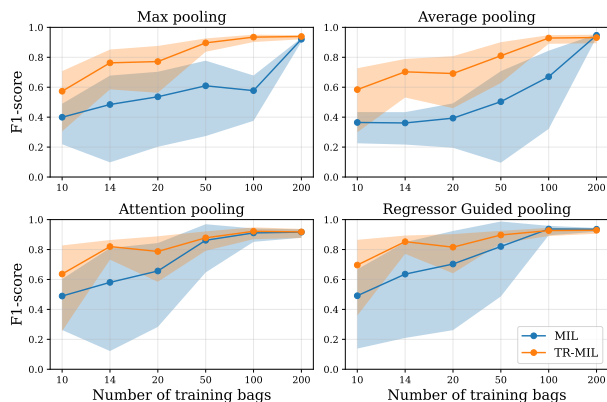
accounting for up to 20% of the instances within the bag.

Models. We use a deep instance encoder architecture introduced by Ilse et al. (2018) (see Table 5 for details). It consists of two convolutional layers with a kernel size of 5, a stride of 1, and ReLU activation functions. These layers generate 20 and 500 feature maps, respectively. This is followed by a fully-connected layer. The output from this encoder is a 500-dimensional feature vector, which then undergoes further processing in the aggregation function. The attention network comprises two linear layers, resulting in a final output dimension of 128 followed by 1. The topological signature of input instances is calculated on image space and latent space, applying pixel-wise Euclidean distance of instance images and latent feature vectors (Figure 1).

Results. We evaluate the effectiveness of topological regularization on three aggregation functions in MIL, max pooling, average pooling, attention-based pooling, which serves as the baseline for numerous studies in the field (Ilse et al., 2018), in addition to the regressor-guided pooling technique, recognized as the state-of-the-art (Du et al., 2023). We analyze the average F1-score and its standard deviation for different numbers of training bags (Figure 3) and bag sizes (Figure 8) over five runs on MIL-MNIST and MIL-FashionMNIST datasets. Without topological regularization, models trained with few training bags perform poorly, akin to random guessing, due to overfitting (Learning curves are shown in Figure 4). Adding topological regularization provides a reasonable complexity for the encoder to resolve overfitting and lets the encoder learn a more meaningful latent representation of data. Consequently, it improves the MIL model performance across both datasets. Notably, topological regularization narrows the performance gap between basic aggregations of max pooling and average pooling compared to advanced techniques of attention and regressor-guided pooling. This demonstrates the crucial role



(a) MIL-MNIST



(b) MIL-FashionMNIST

Figure 3: TR-MIL outperforms MIL models irrespective of the aggregation function when subjected to scarce training data. For each number of training bags, the average and standard deviation for the F1-score in 5 runs over bag sizes of 10, 50, and 100 (in total 15 runs) is reported.

of accounting for a bag’s topological structure in enhancing MIL classification, surpassing the impact of the aggregation function, as evidenced in our toy experiment.

5.3. Anemia Classification

The diagnosis of anemia relies on presence of the minority red blood cells in a patient’s blood sample that shows morphological features associated with the disease. Anemia disorders lead to various aberrant shapes such as sickle-shaped (SCD), crumpled or perforated (thalassemia), star-shaped (Xero), or even spherical (HS) cells. These deformations can manifest with varying degrees of severity and in different proportions, while it is also possible for other cell types unrelated to anemia conditions to coexist. Detecting the hallmark cells indicative of anemia poses a significant challenge due to substantial variability in expert opinions. This makes the *manual* annotation of blood samples for supervised model

training a laborious and costly endeavor (Kazeminia et al., 2022). Lacking cell-level annotations, MIL is used in this context by treating cells as instances and blood samples as bags, with anemia types assigned to each blood sample (Lu et al., 2020).

This dataset consists of 521 microscopy images of blood samples obtained from patients who underwent various treatments at different times. Each sample comprises 4 to 12 images, each containing 12 to 45 cells. The data is distributed among five classes, i.e., (i) Sickle Cell Disease (SCD) with 13 patients and 170 samples, (ii) Thalassemia with only 3 patients and 25 samples, (iii) Hereditary Xerocytosis with 9 patients and 56 samples, (iv) Hereditary Spherocytosis (HS) with 13 patients and 89, as well as (v) healthy control group consisting of 33 individuals and 181 samples. Given the rarity of disease samples in anemia, the dataset for the 5-class Anemia classification task is exhibiting data scarcity of training bags, making its classification challenging. Following previous research, we implement a patient-centric approach by dividing the dataset into three equivalent folds. This division allocates two folds for training and reserves one for test.

In this application, Kazeminia et al. (2022) introduces the state-of-the-art MIL approach, introducing anomaly scores derived from the Mahalanobis distance to a Gaussian mixture model for detecting negative instances in anemia classification. However, the effectiveness of this method is limited by the encoder’s capacity to map negative instances without a direct learning signal.

In addition to data scarcity, the anemia dataset introduces an inherent ambiguity within the dataset: Blood samples may contain a low deformed cell ratio that falls below a specified threshold to identify a disorder. Such data introduces a significant challenge for attention-based and anomaly-aware pooling techniques, as they do not conform to the fundamental assumptions of these mechanisms. Consequently, it is not just the presence of positive instances that is critical, but also their *proportion* in the data. We anticipate that geometry and topology can capture this nuanced information, helping us overcome this challenge. Consistent with prior experiments, for a fair comparison, we apply topological regularization to this architectures (Kazeminia et al., 2022). In previous works, the instance encoder contains 3 convolutions followed by 2 ReLu and Tanh activation functions, followed by 2 linear layers to obtain a latent representation of instances in a 500-dimensional space. The instance encoder’s input is $4 \times 4 \times 256$ features extracted by a frozen encoder trained in a cell segmentation network. However, in our experiments, we capture the topological signature of each bag directly from the image data space and the 500-dimensional latent space. We posit that features extracted by the segmentation model, irrespective of the cell type, may lack crucial shape

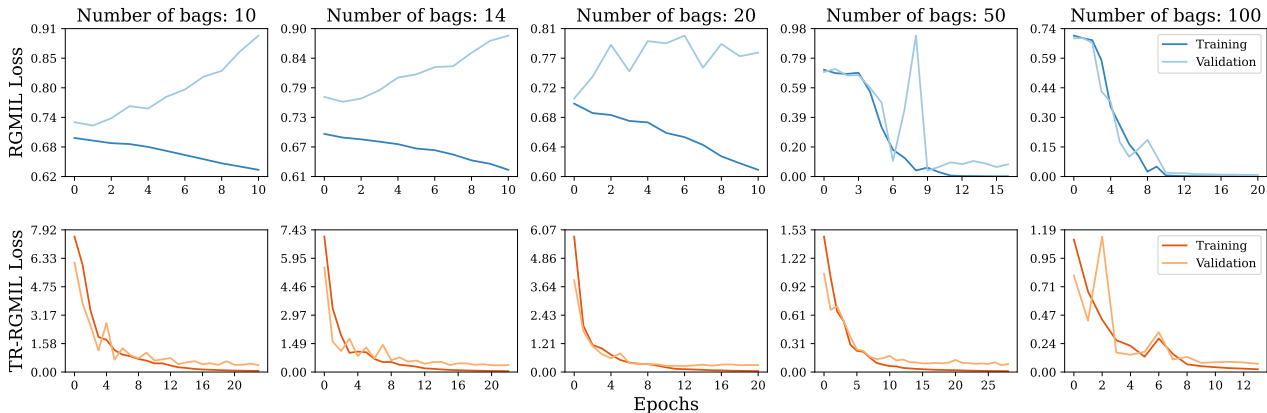


Figure 4: Topological regularization enhances the RGMIL model generalizability for scarce training data. Each column shows learning curves of models trained with 10 bags, each containing 10 instances on average.

Table 2: Topological regularization improves classification performance for all pooling strategies for Anemia classification. We apply it to different MIL methods with average/max pooling, attention-based pooling (Sadafi et al., 2020), and anomaly-aware pooling (Kazeminia et al., 2022). Numbers show the average classification performance along with the standard deviation from 3 cross-validation and 3 runs. Best performance is indicated by bold text. Additionally, for each pooling method, we compare the classification performance without (X) and with (✓) topological regularization, and the winner is underlined for clarity.

| | Average pooling | | Anomaly pooling | | Attention pooling | | Max pooling | |
|----------------------------|-----------------|--------------------------|-----------------|------------------|-------------------|------------------|-------------|------------------|
| Topological regularization | X | ✓ | X | ✓ | X | ✓ | X | ✓ |
| Accuracy | 72.25±7.0 | <u>81.29±2.5</u> | 77.85±3.7 | <u>79.50±1.2</u> | 73.72±3.8 | <u>77.76±1.6</u> | 64.33±5.8 | <u>71.44±5.6</u> |
| F1-Score | 70.47±7.4 | <u>80.28±3.1</u> | 76.69±4.0 | <u>77.01±1.8</u> | 72.38±3.8 | <u>74.69±1.6</u> | 62.96±5.0 | <u>68.77±5.4</u> |
| AUROC | 89.88±2.7 | <u>93.72±4.4</u> | 89.05±4.3 | <u>90.89±2.5</u> | 91.58±3.0 | <u>91.88±2.5</u> | 84.83±2.8 | <u>89.73±3.1</u> |
| Recall | 59.68±7.8 | <u>65.12±5.0</u> | 63.24±3.2 | <u>65.99±3.3</u> | 59.31±6.4 | <u>60.42±2.3</u> | 52.77±8.6 | <u>53.75±4.7</u> |
| Precision | 61.77±7.1 | <u>79.06±12.0</u> | 67.36±4.5 | <u>69.67±4.6</u> | 64.89±4.9 | <u>73.24±7.9</u> | 52.86±9.6 | <u>63.43±7.5</u> |

information and thus potentially manipulate the topology of the bag (see Table 6).

Following common practice in medical and biomedical evaluations, we employ five standard evaluation metrics: Accuracy, F1-Score, Area Under the Receiver Operating Characteristic Curve (AUROC), Precision, and Recall. All metrics are macro-weighted because of the dataset imbalance.

Results. Table 2 shows that topological regularization improves the performance of MIL models using *all* aggregation functions, resulting in higher mean performance and often resulting in reduced variance. Notably, topologically regularized MIL with *average pooling* surpasses other aggregation schemes. This aligns with our findings from experiments on synthetic datasets, where we observe that topological regularization particularly narrowing the gap between performance of the MIL employing different ag-

gregation functions. The inherent ambiguity in the anemia dataset for MIL suggests that enhancing instance projection in latent space via average pooling is more effective than attention pooling, as it better captures the ratio of positive instances. Without topological regularization, scarce training data impede the instance encoder from generating meaningful, generalizable latent representations. However, integrating topological inductive bias into the latent space mitigates these challenges, significantly improving model performance.

Instance-level analysis. We evaluate the influence of topological regularization on the instance-level explanation of the anomaly-aware MIL approach. Figure 5 shows anomaly scores achieved with and without topological regularization. Without topological regularization, we observe a notable inconsistency: the anomaly detector assigns different anomaly scores to visually similar instances. This inconsistency is

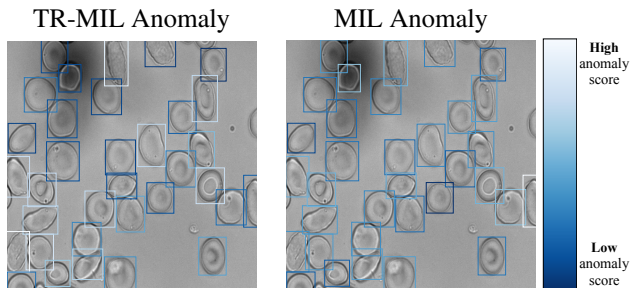


Figure 5: Topological regularization enhances the model’s ability to identify disease-relevant cells more effectively. TR-MIL Anomaly results in more uniform anomaly scores for deformed cells, in contrast to the varied scores resulting from MIL Anomaly.

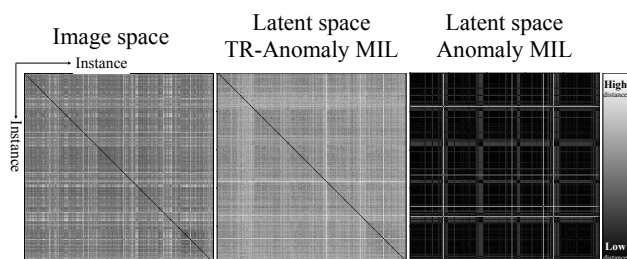


Figure 6: Heatmaps depicting distances between instance images (left), instance latent vectors estimated by topologically-regularized anomaly-aware MIL (middle), and instance latent vectors estimated by anomaly-aware MIL (right), all of which belong to the same bag. Our topological regularization ensures that the model preserves the topological characteristics of the image space in the latent spaces, resulting in latent spaces that resemble the original high-dimensional image space more closely.

mitigated when topological regularization is applied. This is an important aspect of our analysis, revealing a challenge in the model’s ability to evaluate similar data points uniformly and demonstrating the effectiveness of topological regularization in enhancing the model’s explainability. Further illustrating this point, we visualize the distance matrix of instances within a bag in the input space and compare them with their corresponding matrices in the latent space in scenarios with and without topological regularization in Figure 6. This figure shows that MIL with topological regularization better preserves the distances between bag instances in the latent space projection compared to anomaly-aware MIL without regularization. The figure indicates that, without topological regularization, only a few instances are projected far from the majority, elucidating the observed inconsistency in anomaly scores for deformed shapes.

In addressing potential inquiries regarding our choice of

topological regularization over a distance-preservation-based loss, it’s noteworthy to emphasize the distinct advantages of our approach. Topological regularization loss is particularly robust against noise and highly effective in high-dimensional spaces. It exhibits scale invariance, a critical feature that enables the preservation of the distance pattern of instances within a bag. This level of distance pattern preservation might not be as effectively achieved with a regularization loss focused solely on distance preservation. This aspect underscores the strategic advantage of our chosen method, confirming the efficacy of topological regularization in maintaining the integrity of instance relationships in the latent space, thereby enhancing both the model’s performance and its explainability.

6. Conclusion

We present TR-MIL, a novel approach to MIL frameworks, that leverages geometrical-topological properties of bags. This is achieved by employing a topological regularization loss term within the MIL objective function. Our method ensures that intrinsic geometrical-topological characteristics of bags in the input space are consistently maintained in their latent projections. Testing our approach on numerous datasets, We showed that this preservation leads to substantial improvements in terms of predictive performance and generalization performance, especially when dealing with scarce training data.

As for future research directions, we plan to explore alternative methods for describing image geometry and topology, with a particular focus on cubical complexes that can directly operate on images. Additionally, we aim to investigate the geometrical and topological properties of bag spaces, leveraging recent advances in metric geometry, including the Gromov–Hausdorff distance, which has previously been utilized to characterize shapes in related studies (Chazal et al., 2009).

7. Impact Statement

This paper presents work with the primary goal of advancing the field of Machine Learning in healthcare. We have carefully considered the ethical implications of our methodology and application and have not identified any negative social impact that must be specifically highlighted here.

Acknowledgments

We gratefully acknowledge Anna Bogdanova, Asya Makhro, and Ario Sadafi for providing the biomedical dataset used in this research. Their efforts in collecting and sharing the data have been instrumental in advancing our understanding of this field. The Helmholtz Association supports the present

contribution under the joint research school “Munich School for Data Science - MUDS”. C.M. has received funding from the European Research Council (ERC) under the European Union’s Horizon 2020 research and innovation program (Grant Agreement No. 866411). B.R. is supported by the Bavarian state government with funds from the *Hightech Agenda Bavaria*.

References

- Andrews, S., Tsochantaridis, I., and Hofmann, T. Support vector machines for multiple-instance learning. *Advances in neural information processing systems*, 15, 2002.
- Bubenik, P., Hull, M., Patel, D., and Whittle, B. Persistent homology detects curvature. *Inverse Problems*, 36(2): 025008, 2020.
- Chazal, F., Cohen-Steiner, D., Guibas, L. J., Mémoli, F., and Oudot, S. Y. Gromov–Hausdorff stable signatures for shapes using persistence. *Computer Graphics Forum*, 28(5):1393–1403, 2009.
- Chen, C., Ni, X., Bai, Q., and Wang, Y. A topological regularizer for classifiers via persistent homology. In *International Conference on Artificial Intelligence and Statistics*, pp. 2573–2582, 2019.
- Chen, R. J., Chen, C., Li, Y., Chen, T. Y., Trister, A. D., Krishnan, R. G., and Mahmood, F. Scaling vision transformers to gigapixel images via hierarchical self-supervised learning. In *Proceedings of the IEEE/CVF Conference on Computer Vision and Pattern Recognition*, pp. 16144–16155, 2022.
- Cormen, T. H., Leiserson, C. E., Rivest, R. L., and Stein, C. *Introduction to algorithms*. MIT press, 2022.
- Dietterich, T. G., Lathrop, R. H., and Lozano-Pérez, T. Solving the multiple instance problem with axis-parallel rectangles. *Artificial intelligence*, 89(1-2):31–71, 1997.
- Du, Z., Mao, S., Zhang, Y., Gou, S., Jiao, L., and Xiong, L. Rgmil: Guide your multiple-instance learning model with regressor. In *Thirty-seventh Conference on Neural Information Processing Systems*, 2023.
- Edelsbrunner, H. and Harer, J. Computational topology: An introduction. *American Mathematical Society*, 9(2): 117–138, 2009.
- Goyal, A. and Bengio, Y. Inductive biases for deep learning of higher-level cognition. *Proceedings of the Royal Society A*, 478(2266):20210068, 2022.
- Hehr, M., Sadafi, A., Matek, C., Lienemann, P., Pohlkamp, C., Haferlach, T., Spiekermann, K., and Marr, C. Explainable ai identifies diagnostic cells of genetic aml subtypes. *PLOS Digital Health*, 2(3):e0000187, 2023.
- Hensel, F., Moor, M., and Rieck, B. A survey of topological machine learning methods. *Frontiers in Artificial Intelligence*, 4, 2021.
- Horn, M., De Brouwer, E., Moor, M., Moreau, Y., Rieck, B., and Borgwardt, K. Topological graph neural networks. In *International Conference on Learning Representations (ICLR)*, 2022. URL <https://openreview.net/forum?id=oxxUMeFwEHd>.
- Huang, S., Liu, Z., Jin, W., and Mu, Y. Bag dissimilarity regularized multi-instance learning. *Pattern Recognition*, 126:108583, 2022.
- Ilse, M., Tomczak, J., and Welling, M. Attention-based deep multiple instance learning. In *International conference on machine learning*, pp. 2127–2136. PMLR, 2018.
- Kazemina, S., Sadafi, A., Makhro, A., Bogdanova, A., Albarqouni, S., and Marr, C. Anomaly-aware multiple instance learning for rare anemia disorder classification. In *25th International Conference on Medical Image Computing and Computer Assisted Intervention (MICCAI)*, pp. 341–350. Springer, 2022.
- Li, B., Li, Y., and Eliceiri, K. W. Dual-stream multiple instance learning network for whole slide image classification with self-supervised contrastive learning. In *Proceedings of the IEEE/CVF conference on computer vision and pattern recognition*, pp. 14318–14328, 2021.
- Lu, C., Han, B., Liu, Y., Niu, G., Zhang, R., Li, E., Zhou, Y., and Zhang, S. Clinical-grade computational pathology using weakly supervised deep learning on whole slide images. *Nature Medicine*, 26(9):1301–1309, 2020.
- Moor, M., Horn, M., Rieck, B., and Borgwardt, K. Topological autoencoders. In *International Conference on Machine Learning*, pp. 7045–7054, 2020.
- Sadafi, A., Makhro, A., Bogdanova, A., Navab, N., Peng, T., Albarqouni, S., and Marr, C. Attention based multiple instance learning for classification of blood cell disorders. In *23rd International Conference on Medical Image Computing and Computer Assisted Intervention (MICCAI)*, pp. 246–256. Springer, 2020.
- Shao, Z., Bian, H., Chen, Y., Wang, Y., Zhang, J., Ji, X., et al. Transmil: Transformer based correlated multiple instance learning for whole slide image classification. *Advances in neural information processing systems*, 34:2136–2147, 2021.
- Sheehy, D. R. Linear-size approximations to the vietoris–rips filtration. *Discrete & Computational Geometry*, 49(4):778–796, 2013. doi: 10.1007/s00454-013-9513-1.

- Sheehy, D. R. The persistent homology of distance functions under random projection. In *Proceedings of the thirtieth annual symposium on Computational geometry*, pp. 328–334, 2014.
- Turkes, R., Montufar, G., and Otter, N. On the effectiveness of persistent homology. In *Advances in Neural Information Processing Systems*, 2022.
- Vandaele, R., Kang, B., Lijffijt, J., Bie, T. D., and Saeys, Y. Topologically regularized data embeddings. In *International Conference on Learning Representations*, 2022.
- von Rohrscheidt, J. and Rieck, B. Topological singularity detection at multiple scales. In Krause, A., Brunskill, E., Cho, K., Engelhardt, B., Sabato, S., and Scarlett, J. (eds.), *Proceedings of the 40th International Conference on Machine Learning (ICML)*, number 202 in Proceedings of Machine Learning Research, pp. 35175–35197. PMLR, 2023.
- Wagner, A., Solomon, E., and Bendich, P. Improving metric dimensionality reduction with distributed topology, 2021. [arXiv:2106.07613](https://arxiv.org/abs/2106.07613).
- Wagner, S. J., Reisenbüchler, D., West, N. P., Niehues, J. M., Zhu, J., Foersch, S., Veldhuizen, G. P., Quirke, P., Grabsch, H. I., van den Brandt, P. A., et al. Transformer-based biomarker prediction from colorectal cancer histology: A large-scale multicentric study. *Cancer Cell*, 41(9): 1650–1661, 2023.
- Waibel, D. J. E., Atwell, S., Meier, M., Marr, C., and Rieck, B. Capturing shape information with multi-scale topological loss terms for 3D reconstruction. In *25th International Conference on Medical Image Computing and Computer Assisted Intervention (MICCAI)*, pp. 150–159, 2022.
- Xiao, H., Rasul, K., and Vollgraf, R. Fashion-mnist: a novel image dataset for benchmarking machine learning algorithms. *arXiv preprint arXiv:1708.07747*, 2017.
- Yan, Y., Wang, X., Guo, X., Fang, J., Liu, W., and Huang, J. Deep multi-instance learning with dynamic pooling. In *Asian Conference on Machine Learning*, pp. 662–677. PMLR, 2018.
- Zhang, H., Meng, Y., Zhao, Y., Qiao, Y., Yang, X., Coupland, S. E., and Zheng, Y. Dtf-d-mil: Double-tier feature distillation multiple instance learning for histopathology whole slide image classification. In *Proceedings of the IEEE/CVF Conference on Computer Vision and Pattern Recognition*, pp. 18802–18812, 2022.
- Zhao, L., Yuan, L., Hao, K., and Wen, X. Generalized attention-based deep multi-instance learning. *Multimedia Systems*, 29(1):275–287, 2023.

A. Appendix

A.1. Experimental MIL Architectures

| Component | Configuration |
|------------------|--|
| Input channels | 100 |
| Instance encoder | linear(100 → 64), ReLU, linear(64 → 2), ReLU |
| Latent dimension | 2 |
| Pooling | regressor guided pooling |
| Classifier head | linear (100 → 2) |
| Loss | BCEWithLogitsLoss and TopoRegLoss |
| Optimizer | Adam (lr: 0.0005) |
| λ | 0.005 |

Table 3: Architecture of the MIL model for toy experiment.

The RGMIL (Du et al., 2023) model uses regressor guided pooling technique. In this model, the regressor (with parameters W and B) calculates the binary probability value of instance latent representation z_i as

$$(p_i^+, p_i^-) := W^T z_i + B, \quad (6)$$

where p_i^+ and p_i^- show the probability of instance z_i to belong to the positive or negative class. Then it gets the difference between these two achieved probabilities,

$$p_i = p_i^+ - p_i^-, \quad (7)$$

normalizes the result

$$\omega_i = \frac{p_i - \mathbb{E}[p_i]}{\sqrt{\text{Var}(p_i)}}, \quad (8)$$

and applies softmax on it

$$\alpha_i = \frac{\exp(\omega_i)}{\sum_{j=1}^n \exp(\omega_j)}. \quad (9)$$

where, α_i specifies the pooling weight of z_i . Then the latent of bag is

$$\zeta_{b_m} = \sum_{i=1}^n \exp(\alpha_i z_i). \quad (10)$$

Table 3 specifies more details of the MIL architecture we developed to classify toy dataset.

| Components | Elephant, Fox, Tiger | Musk1, Musk |
|------------------|--|-------------|
| Input channels | 230 | 166 |
| Instance encoder | linear(231, 512), ReLU, linear(512, 512), ReLU | |
| Latent Dimension | 512 | |
| Pooling | regressor guided pooling | |
| Classifier head | linear (512 → 2) | |
| Loss | BCEWithLogitsLoss and TopoRegLoss | |
| Optimizer | Adam (lr: 0.00005, Betas: [0.9, 0.999]) | |
| Max Epochs | 40 | |
| λ | 0.05 | |

Table 4: Architecture of the MIL Model for Benchmarks

Table 4 shows the settings of this architecture.

| Parameter | Max Pooling | Average Pooling | Attention Pooling | RGP Pooling |
|----------------------------|---|-----------------|-------------------|------------------|
| Pooling | Max | Average | Attention | regressor guided |
| In Dimension | 28 × 28 | | | |
| Input channel | 1 | | | |
| Instance encoder | linear(1→20), ReLU, linear(20→50), ReLU, linear(50→500), ReLU | | | |
| Latent dimension | 500 | | | |
| Attention latent dimension | 128 | | | |
| Linear Layer | 500 × 2 | | | |
| Loss | BCEWithLogitsLoss and TopoRegLoss | | | |
| Optimizer | Adam (LR: 0.005) | | Adam (LR: 0.0005) | |
| Batch Size | 1 | | | |
| Max Epochs | 100 | | | |

Table 5: General architecture and configurations of TR-MIL Model for synthetic datasets over different pooling strategies. The value λ is not reported here as it differs between datasets, training budgets, and bag sizes. Please find its relevant value in the source code.

For synthetic data we employed same architecture for both MIL-MNIST and MIL-FashionMNIST datasets. We explored different aggregation functions containing max pooling

$$\zeta_{b_m} = \max_{i \leq n} z_i, \quad (11)$$

average pooling

$$\zeta_{b_m} = \frac{\sum_{i=1}^n z_i}{n}, \quad (12)$$

and attention pooling with parameters W and V

$$\zeta_{b_m} = \sum_{i=1}^n a_i z_i, \quad (13)$$

where

$$a_i = \frac{\exp(W^T \tanh(V z_i^T))}{\sum_{i=1}^n \exp(W^T \tanh(V z_i^T))}. \quad (14)$$

Table 5 shows the settings of this architecture.

For anemia classification we followed the architecture of the state of the art in this application (Kazeminia et al., 2022) (Table 6). This method introduced anomaly score to be considered in addition to attention values to estimate the importance of each instance. To this end the distribution of negative instances is estimated from negative bags by fitting a gaussian mixture model on their latent representation. The anomaly score of each instance latent z_i is calculated as

$$d_i = \sqrt{(z_i - \mu)^T \Sigma^{-1} (z_i - \mu)}, \quad (15)$$

where μ and Σ are mean and covariance of the fitted GMM on negative distribution. Then the pooling weight of the instance is calculated as a linear combination of attention score a_i and anomaly score d_i . With this the bag latent is

$$\zeta_{b_m} = \sum_{i=1}^n (W_{D_i} d_i + W_{A_i} a_i) z_i. \quad (16)$$

The other consideration of this approach is the formulation of $Loss_{class}$ with a dual classifier head (Sadafi et al., 2020) that comprises a bag classifier head and an instance classifier head. The bag classifier head is trained using a cross-entropy loss function L_{bag} , calculated as the difference between the predicted bag label and the corresponding ground truth label for the bag. The instance classifier head is trained using a cross-entropy loss function $L_{Instance}$ that utilizes the noisy labels of instances as the repeated labels of the bag for all instances. The final MIL classification loss is calculated as

$$L_{class} = (1 - \gamma)L_{bag} + \gamma L_{Instance}, \quad (17)$$

where γ is a coefficient that decreases as with epoch number increasing.

Topologically Regularized Multiple Instance Learning to Harness Data Scarcity

| Parameter | Max Pooling | Average Pooling | Aux Attention | Anomaly Detection |
|--------------------------|---|-----------------|---|-------------------|
| Image dimentions | 64 × 64 | | | |
| Image channels | 1 | | | |
| Features channels | 256 | | | |
| Instance encoder | Conv2D(256→301), ReLU, Conv2D(301→500), ReLU, Conv2D(500→650), Tanh, Linear(650→500)) | | | |
| Latent Dimension | 500 | | | |
| Instance classifier head | - | | Linear(500 → 500), Linear(500 → 5) | |
| Pooling | Max | Average | Attention | Anomaly |
| Attention layer | - | | Linear(500→128), Tanh, Linear(128→1) | |
| Bag classifier head | Linear(500 → 2) | | | |
| Loss | bag CrossEntropyLoss and TopoRegLoss | | CrossEntropyLoss (bag and instance) and TopoRegLoss | |
| Optimization | Adam (lr=0.0005) | | | |
| Learning Rate | 0.0005 | | | |
| Max Epochs | 300 | | | |
| Early Stopping | patience: 50 | | | |
| Image input channels | 1 | | | |
| λ | 0.005 | | | |

Table 6: Configuration of MIL model for anemia classification with different pooling strategies

A.2. Lurning curves on Benchmarks

The RGMIL model tends to overfit when performing on benchmark datasets, given their limited data size. Figure 7 displays the learning curves of training RGMIL alongside TR-RGMIL. The introduction of topological regularization addresses overfitting in RGMIL and results in a significant improvement in its classification performance.

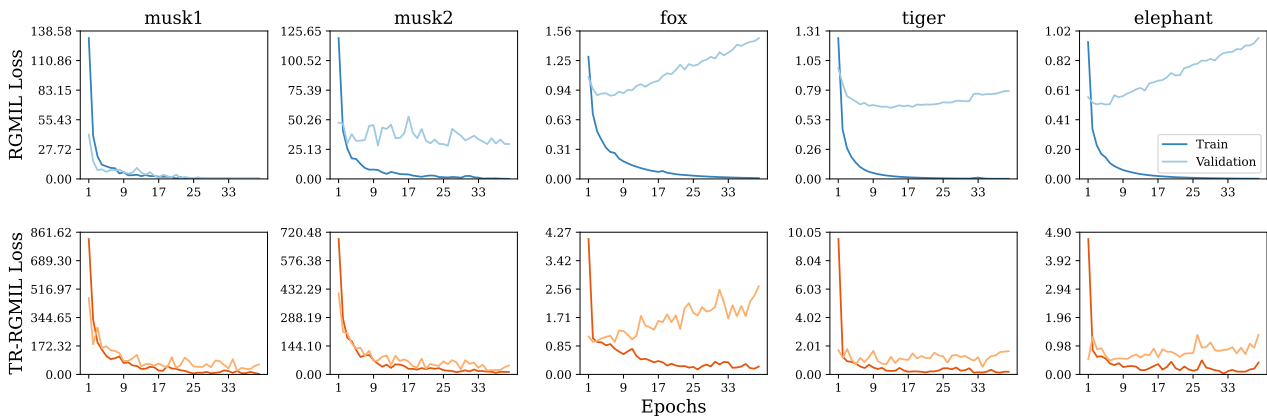


Figure 7: Topological regularization enhances RGMIL model generalizability for Benchmarks. Each column shows learning curves achieved by a MIL benchmark dataset.

A.3. Detailed performance on synthetic dataset

Table 8 distinctly illustrates how topological regularization addresses this issue in MIL employing both average and attention aggregation functions. This effect is particularly pronounced with smaller bags, leading to improved robustness (lower variance across multiple runs) and higher accuracy on average.

Furthermore, the figure effectively highlights the advantages of the attention mechanism over average pooling in enhancing MIL performance, especially when trained with limited data. However, for a small amount of training bags, topological regularization improves performance by generating more accurate and robust results.

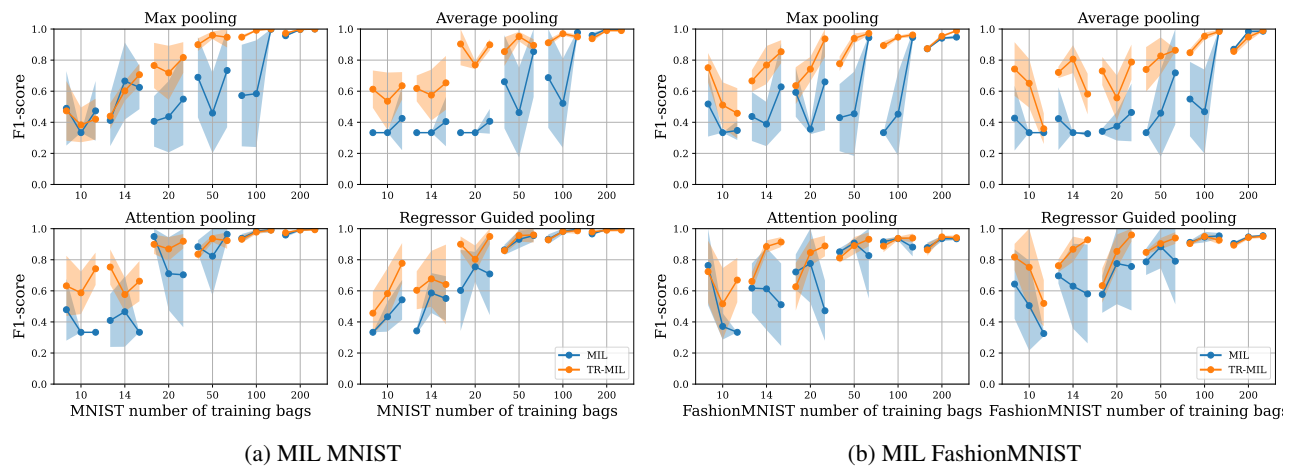


Figure 8: TR-MIL outperforms MIL models irrespective of the aggregation function when subjected to a limited amount of training bags. For each number of training bags, the average and standard deviation for the F1-score of the model’s performance in 5 runs for each bag size of 10, 50, and 100 (in total 15 runs) is shown.